Membrane/Microtubule Tip Attachment Complexes (TACs) Allow the Assembly Dynamics of Plus Ends to Push and Pull Membranes into Tubulovesicular Networks in Interphase *Xenopus* Egg Extracts

Clare M. Waterman-Storer,*§ Jennifer Gregory,*‡ Stephen F. Parsons,*‡ and E. D. Salmon*‡

*Marine Biological Laboratory, Woods Hole, Massachusetts 02543; ‡Department of Biology, University of North Carolina, Chapel Hill, North Carolina 27599-3280; and §Department of Animal Biology, University of Pennsylvania School of Veterinary Medicine, Philadelphia, Pennsylvania 19104-6046

Abstract. We discovered by using high resolution video microscopy, that membranes become attached selectively to the growing plus ends of microtubules by membrane/microtubule tip attachment complexes (TACs) in interphase-arrested, undiluted, *Xenopus* egg extracts. Persistent plus end growth of stationary microtubules pushed the membranes into thin tubules and dragged them through the cytoplasm at the ~20 μm/min velocity typical of free plus ends. Membrane tubules also remained attached to plus ends when they switched to the shortening phase of dynamic instability at velocities typical of free ends, 50–60 μm/min. Over time, the membrane tubules contacted and fused with one another along their lengths, forming a polygonal network much like the distribution of ER in cells. Several components of the membrane networks formed by TACs were identified as ER by immunofluorescent staining using antibodies to ER-resident proteins. TAC motility was not inhibited by known inhibitors of microtubule motor activity, including 5 mM AMP-PNP, 250 μM orthovanadate, and ATP depletion. These results show that membrane/microtubule TACs enable polymerizing ends to push and depolymerizing ends to pull membranes into thin tubular extensions and networks at fast velocities.

THE microtubule cytoskeleton provides a structural basis for the transport and positional maintenance of tubulovesicular membranous organelles in the cytoplasm of eukaryotic cells. In living cells, the tubulovesicular membrane networks of both the ER (Terasaki et al., 1984; Lee and Chen, 1988; Terasaki and Reese, 1994) and Golgi apparatus (Cooper et al., 1990) have been observed to form through a process whereby single membrane tubules advance towards the cell periphery, contact other advancing tubules, and fuse to form junctions and polygonal networks. The direction of nascent membrane tubule extension and branching is often correlated with the positions of single microtubules (Terasaki et al., 1986; Dailey and Bridgman, 1989; Lee et al., 1989; Terasaki and Reese, 1994).

Two models have been proposed to explain the observed colinear growth and distribution between microtubules and membrane tubules in living cells. The first is based on the involvement of microtubule motor proteins, such as the kinesins or cytoplasmic dynein. In this model, either the microtubule serves as a stationary track upon which the membrane-attached motors move, or the membrane forms a static link to a preexisting microtubule, and the attached membrane is translocated by microtubule-microtubule gliding generated by motor activity between microtubules. In support of this, several investigators (Dabora and Sheetz, 1988; Vale and Hotani, 1988; Allan and Vale, 1991, 1994) have shown that dynamic ER-like membrane tubule networks form in vitro by microtubule or membrane gliding mechanisms when crude organelle fractions are mixed with cytosolic extracts and taxol stabilized microtubules in the presence of ATP. In an alternate model, forces are not generated by the activity of microtubule motor proteins. Instead, membrane tubules may be extended by their attachment to the tips of elongating microtubules, and force is provided by microtubule polymerization itself (as suggested by Dailey and Bridgman, 1989). In this case, a specialized membrane attachment would be required to couple a membrane to the dynamic end of a microtubule during the addition and removal of tubulin subunits, not unlike the type of attachment that forms between a kinetochore and the tip of a spindle microtubule during the chromosomal movements in mitosis (reviewed by Rieder and Salmon, 1994).

In this paper, we provide the first direct evidence that cellularly derived membranes selectively attach to dynamic plus ends of microtubules by membrane/microtu-

Address correspondence to E. D. Salmon, Dept. of Biology, University of North Carolina, Chapel Hill, NC 27599-3280. Tel.: (919) 962-2265. Fax: (919) 962-1625.

bule tip attachment complexes (TACs)[1]. The interactions between individual microtubule ends and membrane vesicles were recorded and analyzed using high resolution video-enhanced differential interference contrast microscopy (VE-DIC) in undiluted interphase cytoplasmic extracts of *Xenopus* eggs. Our results show that membrane/microtubule TACs push and pull membranes into tubules and polygonal networks by the polymerization and depolymerization of microtubules at the plus end TAC attachment site, even under conditions that inhibit microtubule-based motor activity.

Materials and Methods

Preparation of Interphase-arrested Xenopus Extracts

Undiluted cytoplasmic extracts of *Xenopus* eggs were prepared according to the method of Murray (1991). Meiotically arrested extracts were induced into interphase by a 40-min incubation at 20°C in the presence of 50 μM emetine and 0.3 mM $CaCl_2$. The extract was then clarified via a 100,000-*g* spin in a TL-100 rotor (Beckman Instrs., Inc., Fullerton, CA) for 30 min at 22°C, and the supernatant was frozen in liquid nitrogen and stored at −80°C until use.

Membrane Motility Assays

Interphase-arrested *Xenopus* extract, made 1 mM in both GTP and $MgCl_2$, was introduced into a ~10-μl capacity simple flow chamber (assembled from a slide, a 22 × 22-mm no. 1 coverslip and two parallel strips of 70-μm-thick double-stick tape, which formed a 4-mm-wide channel). The chamber was sealed with valap and microtubule growth dynamics and membrane network formation were observed just below the plane of the coverslip by VE-DIC. For most experiments, flow chambers were perfused with *Stronglyocentratus purpuratus* axonemes (Bell et al., 1982) in XB buffer (100 mM KCl, 0.1 mM $CaCl_2$, 1 mM $MgCl_2$, 50 mM sucrose, 10 mM Hepes, pH 7.7) before adding extract and observing the formation of membrane networks. In some experiments, extracts were diluted 1:3 in acetate buffer (Allan and Vale, 1994) (100 mM potassium acetate, 3 mM magnesium acetate, 5 mM EGTA, 150 mM sucrose and 10 mM Hepes, pH 7.4) and made 1 mM in GTP and $MgCl_2$ before introduction into the chamber. When Mg^{2+} AMP-PNP or sodium orthovanadate were used in both diluted and undiluted extracts, they were added from 100 and 89 mM stock solutions, respectively. To deplete ATP from the undiluted extracts, 50 μg/ml hexokinase (Calbiochem-Novabiochem, La Jolla, CA), 200 μM AP_5A (P^1P^5-di(adenosine-5′)pentaphosphate) and 1 mM glucose were added and the extract was incubated ~30 min at room temperature.

Microscopy and Data Analysis

Motility was monitored by VE-DIC at room temperature with a Nikon Microphot FXA microscope (Nikon Inc., Melville, NY) equipped with a DIC aplanatic achromat 1.4 oil condenser and a 60× 1.4 oil planapochromat DIC objective and 4× projection magnification to the video camera. Illumination was provided by a 200 W metal halide lamp (Nikon) and relayed into the microscope through a 546 ± 20-nm bandwidth filter by a liquid light guide (Nikon). Images were collected by a Hamamatsu Newvicon C-2400 camera and contrast enhancement, background subtraction and four frame averaging were performed by a Hamamatsu Argus-10 image processor prior to recording the images in real time on a Panasonic S-VHS recorder (model AG-6750AP; Panasonic, Secaucus, NJ). Average rates of microtubule growth and shortening were calculated directly from video tapes in real time by regression analysis of microtubule length changes over time using a PC-based analysis system (Walker et al., 1988). Epifluorescent images were recorded using a multimode digital fluorescence microscope system (Salmon et al., 1994) using a Nikon 60× 1.4 Plan Apochromat objective and 1.0× projection magnification to a Hammamatsu C4880 cooled CCD camera (Hammamatsu Corp, Bridgewater, NJ). Images were captured in digital format from the camera or from video tapes using a Metamorph image processing system (Universal Imaging Corp., Westchester, PA). Image contrast enhancement and "sharpening" convolutions were performed using Adobe Photoshop software, and micrographs were printed on a dye sublimation printer (Tektronix Phaser II SDX; Textronix S. p. A., Milan) with a four color ribbon.

Immunocytochemistry

Xenopus extracts and crude rat pancreatic RER fractions (provided by C. Nicchita, Duke Univ., Durham, NC) were fractionated by SDS-PAGE, electroblotted to nitrocellulose in transfer buffer (50 mM CAPS, 20% MeOH, 0.075% SDS, pH 11.5) and the blots probed with rabbit polyclonal antibodies (kind gift of C. Nicchita) specific to the resident ER protein ribophorin I (Rosenfeld et al., 1984), an anti-peptide antibody to the NH_2-terminal 12 amino acids of sec61p (Gorlich et al., 1992) or an anti-peptide antibody to the NH_2-terminal 12 amino acids of BiP (GRP78) (Munro and Pelham, 1986). Primary antibodies were localized using HRP-conjugated secondary antibodies and blots developed with 4-chloro-3-napthol. ER-specific antibodies reacted exclusively with single bands in interphase *Xenopus* extract (not shown). To prepare for immunofluorescence localization of ER proteins, *Xenopus* extract was diluted 1:3 in acetate buffer, made 5 mM in AMP-PNP, and then axonemes were added to the flow chamber. Under these conditions, membrane networks formed in close contact with the coverslip and were undisturbed by fluid flow through the chamber. Extract was then added to the chamber, and networks were allowed to form for ~30–60 min. When membrane networks were visible by VE-DIC, acetate buffer was slowly perfused through the chamber to wash out excess cytosol, and this was followed by perfusion with 0.2% glutaraldehyde in acetate buffer. Fixation proceeded for 20 min at room temperature. The coverslips were then removed from the slide and incubated at −20°C for 6 min each in MeOH and then acetone, successively. Coverslips were blocked in PBS containing 1 mg/ml $NaBH_4$ and then in PBS plus 1% normal goat serum and 10% fetal calf serum, before processing for indirect immunofluorescence.

Results

Membrane Tubules and Polygonal Networks Are Formed by Microtubule TACs

To view microtubule/membrane interactions in an environment as close as possible to in vivo conditions, we used undiluted cytoplasmic extracts of *Xenopus* eggs that were blocked in interphase (Murray, 1991). These extracts were clarified of yolk and large membrane aggregates by high-speed centrifigation (100,000 *g* for 30 min) to enable VE-DIC microscopy of individual microtubule assembly dynamics (Parsons, S. F., and E. D. Salmon, manuscript in preparation). The total protein concentration in extracts prepared by this method is near 80 mg/ml and the tubulin concentration is ~20 μM (Parsons, S. F., and E. D. Salmon, manuscript in preparation). Microtubule assembly in the extracts was seeded from axoneme fragments attached to the inner surface of the coverslip. Only plus end growth occurs from axonemes in *Xenopus* cytoplasmic extracts; minus end growth is blocked (Gard and Kirschner, 1987; Belmont et al., 1990). Microtubules grew rapidly in our extracts, (17 ± 4 μm/min (n = 33), Table I), with rare dynamic instability, such that within ~15 min a dense meshwork of long microtubules was established. Spontaneous nucleation occurred more slowly in comparison to the nucleation of plus end growth from axonemes (Belmont et al., 1990; Verde et al., 1992). Although the extracts had been clarified, many membrane vesicles and aggregates were present.

After ~30 min of microtubule assembly, long, thin

1. *Abbreviations used in this paper*: TAC, tip attachment complexes; VE-DIC, video-enhanced differential interference contrast microscopy.

Table I. Rates of Elongation and Shortening for Free Microtubules Plus Ends and Microtubules with Membrane TACs Coupled to Their Plus Ends

	Free MTs	TACs
	(μm/min ± SD)	
Elongation		
Control	17 ± 4 (n = 33)	19 ± 4 (n = 51)
5 mM AMP-PNP	15 ± 2 (n = 14)	22 ± 3 (n = 27)
25 μM $NaV0_4$	27 ± 5 (n = 54)	27 ± 4 (n = 56)
250 μM $NaVO_4$	20 ± 3 (n = 24)	22 ± 2 (n = 36)
ATP depletion	19 + 4 (n = 46)	21 + 6 (n = 93)
Shortening		
5 mM AMP-PNP	58 + 6 (n = 7)	55 + 6 (n = 7)

Undiluted extract was used in all experiments. ATP was depleted from extracts by the addition of 50 μg/ml hexokinase, 200 μM AP_5A and 1 mM glucose. Because catastrophe was so infrequent in control extracts, microtubule shortening rates were only determined in extracts containing AMP-PNP.

membrane tubules were frequently seen attached solely to the tips of microtubules as they extended through the extract at ~19 μm/min (Figs. 1 *a* and 2; Table I). We term the membrane region that binds to the tip of a microtubule a tip attachment complex. By VE-DIC, the TAC is characterized by a bulb-like, refractile, globular domain at the end of the membrane tubule where it attaches to the microtubule tip (Figs. 1 *a* and 2).

These membrane tubules formed when a microtubule end moved through a membrane aggregate or tubule extension, and an attachment between the membrane and the microtubule tip formed (Fig. 2). As the microtubule end moved beyond the aggregate, the attachment remained, and a membrane tubule was extended. Globular membrane aggregates often became stretched out into compliant tubules, more than 50 μm in length, as the microtubule tip pushed the membrane through the extract for many minutes. The formation of membrane tubules was dependent on the presence of microtubules, as depolymerization of microtubules by a 30-min incubation at 4°C caused membrane tubules to disappear. This effect was reversed upon rewarming the slides to 25°C.

The membrane tubules were rough in profile, and typically appeared quite flexible in comparison to microtubules, exhibiting extensive lateral Brownian motion. As forming membrane tubules came into contact with one another along their lengths, they fused, forming three way junctions characteristic of ER networks in living cells and similar to the membrane polygonal networks formed in other in vitro systems (Dabora and Sheetz, 1988; Vale and Hotani, 1988; Allan and Vale, 1991, 1994). After ~90 min, extensive polygonal networks became established (Fig. 1 *b*). The polygonal membrane networks stained with the lipophilic, cationic dye $DiOC_6(3)$ (not shown) and by antibodies to molecules specific for ER including GRP78 (BiP), a 78-kD lumenal ER protein (Munro and Pelham, 1986), ribophorin I, a 66-kD RER oligosaccharyl transferase (Rosenfeld et al., 1984), and sec61p, a 39-kD integral ER membrane protein (Gorlich et al., 1992). Localization with $DiOC_6(3)$ or any of the three antibodies revealed labelling of an extensive polygonal membrane network that resembled ER from living cells (Fig. 1 *c*).

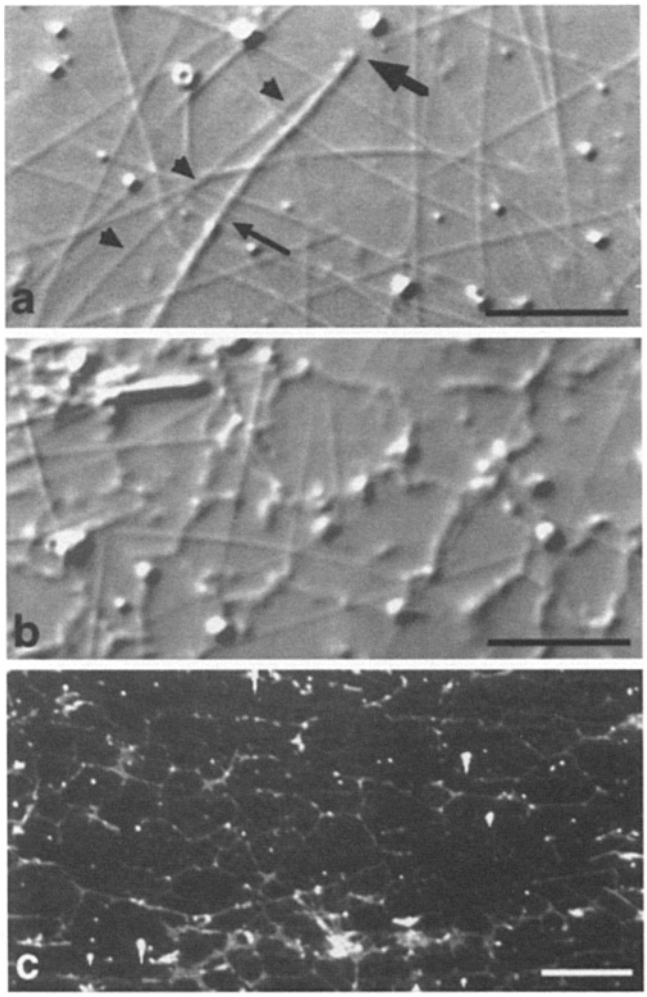

Figure 1. The formation of membrane tubules and polygonal networks in undiluted, clarified interphase arrested *Xenopus* extracts. (*a*) VE-DIC micrograph of an extended tubular membrane (*small arrow*) attached to the tip (*large arrow*) of an individual microtubule (*arrowheads*) seen ~30 min after initiation of microtubule assembly. (*b*) An extensive polygonal tubulovesicular membrane network formed in the extract ~90 min after the initiation of microtubule assembly. (*c*) Fluorescence micrograph of membrane networks. Extract was observed by VE-DIC microscopy for ~90 min until membrane networks formed. The preparation was then fixed and processed for immunofluorescent localization of the ER protein, GRP78, with the BiP antibody. This antibody was localized to the polygonal membrane network. Bars: (*a* and *b*) 5 μm; (*c*) 10 μm.

TACs Are Pushed by Polymerizing Microtubule Plus Ends in the Presence of Inhibitors of Microtubule Motor Activity

Several observations indicated that the formation of membrane tubules and polygonal networks in our undiluted *Xenopus* extracts was mainly produced by microtubule plus end polymerization at the TAC and not by membrane attachment to the ends of microtubules that were gliding along the coverslip surface. We seldom observed membrane tubule gliding along stationary microtubules nor microtubule gliding over the coverslip surface. In addition,

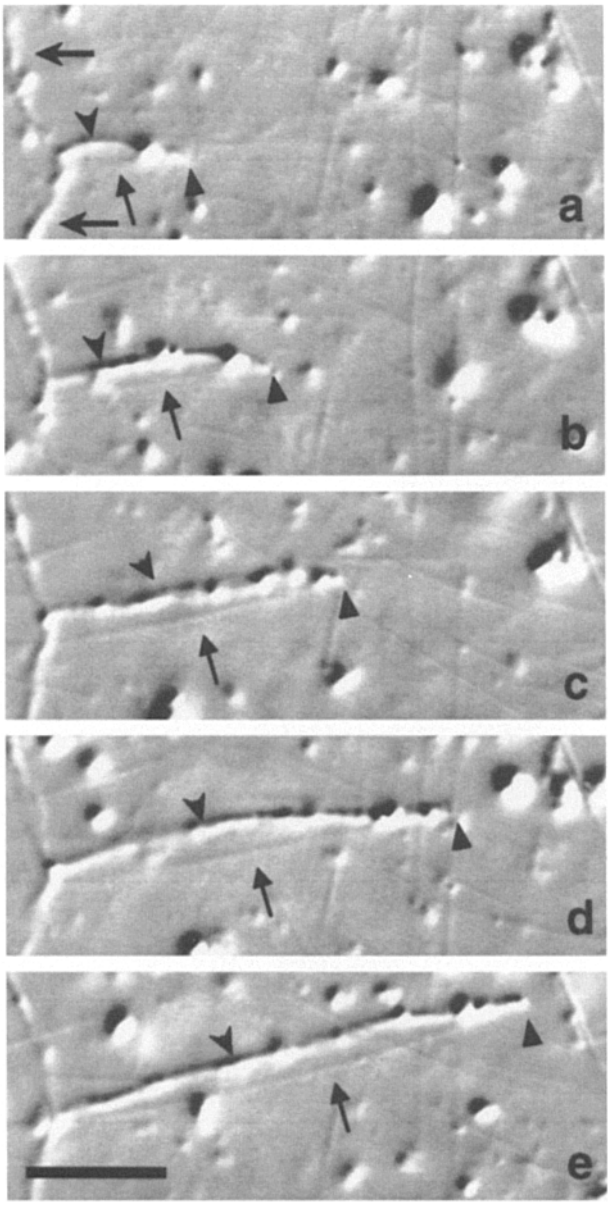

Figure 2. Membrane tubules form by attachment to the tip of a microtubule in undiluted extract. (*a*) A membrane tubule (*small arrowhead*) was formed from a preexisting tubulovesicular membrane (*large arrows*) by attachment solely to the tip (*large arrowhead*) of a single elongating microtubule (*small arrow*). (*b–e*) As the microtubule tip continued to move at ~20 μm/min, its attachment to the membrane remained intact (*large arrowhead*), and the membrane tubule (*small arrowhead*) was pulled out as the microtubule elongated. Time: (*a*) 0 s; (*b*) 12 s; (*c*) 22 s; (*d*) 33 s; (*e*) 41 s. Bar, 5 μm.

the velocity of TAC motility was nearly identical to the velocity of the plus end growth of microtubules nucleated from coverslip-bound axonemes (Table I). After 20 min of microtubule growth, microtubules were hundreds of microns long and some self nucleation had occurred. This made it difficult to track many microtubules from the TAC on the membrane tubule to the nucleation site. However, clear examples were recorded showing membrane tubule attachment to the polymerizing plus ends of microtubules nucleated from coverslip bound axonemes.

As a test of the relative roles of microtubule polymerization and microtubule motor activity in membrane tubule extension, we treated the undiluted extracts with inhibitors of microtubule motor activity (Allan and Vale, 1991). Extracts were either treated with 5 mM AMP-PNP, 25 or 250 μM orthovanadate ion, or ATP was depleted by the addition of 50 μg/ml hexokinase, 200 μM AP_5A (to inhibit conversion of GTP to ATP) and 1 mM glucose. In all cases, small membrane vesicles became statically bound to microtubules and the infrequent microtubule gliding activity seen in control extracts was stopped. In 5 mM AMP-PNP in particular, selfnucleation of microtubule assembly was blocked, and all microtubule assembly occurred from coverslip-bound axonemes. Nevertheless, membrane tubules continued to form by attachment to the tips of growing microtubules over the same time period as in control extracts (Table I). When a vesicle became bound to a microtubule that was actively extending a membrane tubule at its tip, the vesicle remained stationary on the microtubule, while the distance between the vesicle and the advancing microtubule tip increased (not shown), again indicating that the movement of the microtubule tip was due to microtubule plus end polymerization as opposed to microtubule translocation.

To further examine the role of microtubule motor activity within the TAC complex, we compared the kinetics of microtubule plus end growth with and without attached membrane TAC complexes, both in the presence or absence of the inhibitors of microtubule motor activity. Microtubules with attached membranes had growth kinetics that were similar to free ends (Fig. 3). In addition, none of the inhibitors tested produced any significant inhibition of growth velocity, nor did they induce pauses or sudden shifts in velocity for either free or TAC-coupled microtubule ends (Fig. 3 and Table I). In addition, the TACs did not induce any noticable increase in dynamic instability in comparison to unbound ends under the same conditions.

The above results were unexpected based on previous reports that membrane tubule networks are formed in interphase *Xenopus* extracts by membrane-microtubule sliding mechanisms (Allan and Vale, 1991, 1994). In these studies, the extracts were diluted 1:3 with an acetate buffer and membrane tubules were shown to be pulled from endogenous membrane aggregates by making a sliding attachment to the shaft of a preexisting, stationary microtubule. We prepared extracts in an identical fashion to those of Allan and Vale (1991, 1994) (see Materials and Methods). In these acetate buffer-diluted interphase extracts, membrane tubules were extended via motile attachments that glided along microtubules in regions near the coverslip surface, as reported. However, just below the plane of the coverslip, membrane tubules were extended by their attachment to microtubule ends (not shown). Addition of either 5 mM AMP-PNP or 250 μM vanadate inhibited the formation of membrane tubules by gliding, while membrane tubule formation by TAC motility was unaffected (Table II). Thus, two means of microtubule dependent membrane tubule formation can occur simultaneously in *Xenopus* extracts. Microtubule motor inhibitors block the sliding mechanism, while the polymerization driven TAC mechanism remains unaffected.

Table II. Quantification of TAC and Sliding Induced Membrane Tubule Elongation in Extracts Diluted 3:1 in Acetate Buffer

	TACs/4 min	Sliding events/4 min
Control	11 ± 2	7 ± 3
5 mM AMP-PNP	11 ± 2	0 ± 0
250 μM orthovanadate	10 ± 2	2 ± 1

Values were obtained by averaging the number of events (TACs and/or sliding events) recorded in six separate 4-min observation periods.

TACs Remain Attached to Depolymerizing Plus Ends

Microtubule ends in the growth phase of dynamic instability are believed to be stabilized by a terminal cap of straight GTP-tubulin protofilaments, while microtubule ends in the shortening phase have curved GDP-tubulin protofilaments (reviewed by Caplow, 1992; Erickson and O'Brien, 1992; see also Dreschel and Kirschner, 1994). Thus, it was of interest to know whether the membrane TAC complexes stayed bound to plus ends when they switched from growth to shortening. However, in the undiluted extract preparations used in this study, microtubules grew steadily for as long as the preparations retained their ability to form membrane networks, often up to 2 h. We found that addition of 5 mM AMP-PNP to the extracts increased the frequency of catastrophe (the switch from growth to shortening) without altering the normal growth rate of unattached ends (Table I).

Under these conditions, it was apparent that membrane TACs were capable of retaining their attachment to the microtubule tip not only during elongation, but also during catastrophe, shortening, and rescue (the switch from shortening back to growth). During rapid shortening the tubule remained attached to and was pulled back with the shortening end (Fig. 4). In a few cases, microtubule plus ends were observed to go through several cycles of growth and shortening over distances of at least 20–30 μm, while TACs remained attached. The velocity of shortening for ends bound to TACs was 55 μm/min, not significantly different than the 58 μm/min velocities measured for free ends in the AMP-PNP treated extracts (Fig. 3 and Table I) and the 58 μm/min velocities, observed for extracts without AMP-PNP where catastrophe was induced by adding 1 μM porcine brain tubulin (Parsons, S., and E. D. Salmon, unpublished observations). Thus, the membrane/microtubule TACs were functional in both the growth and shortening phases of dynamic instability.

The Dynamic Attachment of Membrane TACs to Microtubule Plus Ends Is Robust

We obtained an estimate of the character and strength of TAC attachment to polymerizing plus ends from the buckling of microtubules. Membrane tubules exerted a compressive force on their attached microtubules. Buckling was usually not significant when plus end growth was resisted only by drag forces on the membrane. However, occasionally a membrane tubule would become stuck to the glass within 10–20 μm of the growing plus end. When this occurred, the membrane tubule became noticably "taut" as the microtubule continued to grow. The stretched, taut condition of the membrane was indicated by a loss of pliance, a reduction in lateral Brownian motion, and the acquisition of a smoother, narrower profile (Fig. 5 *a*). As elongation continued, the stretched membrane tubule bent the tethered microtubule into a short radius of curvature (<20 μm) when objects attached to the glass or the microtubule network inhibited lateral microtubule movement. In some cases, microtubules bowed a full 90–180°, such that membranes were attached at angles of ~90° to the growing microtubule tip axis (Fig 5 *b*). When the limit of TAC attachment force was reached, the membrane tubule snapped off of the microtubule end and shortened

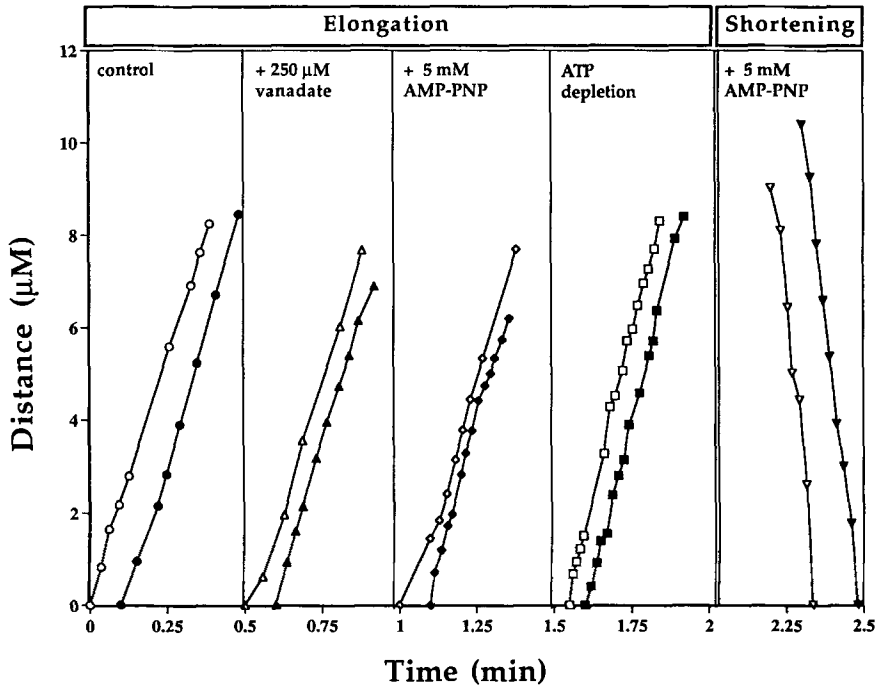

Figure 3. The kinetics of plus end growth and shortening are unaltered by the attachment of a membrane microtubule TAC. Position of the microtubule tips with (*closed symbols*) and without (*open symbols*) TACs was monitored over time. Changes in distance were measured relative to the first data point for each plot and plots were arbitrarily shifted along a single time axis for comparison. The points in each plot are interconnected by straight lines. Deviations from linearity are likely due to inaccuracies in tracking the positions of microtubule ends as they came in and out of focus. Inhibitors of microtubule motor activity were added to undiluted extract.

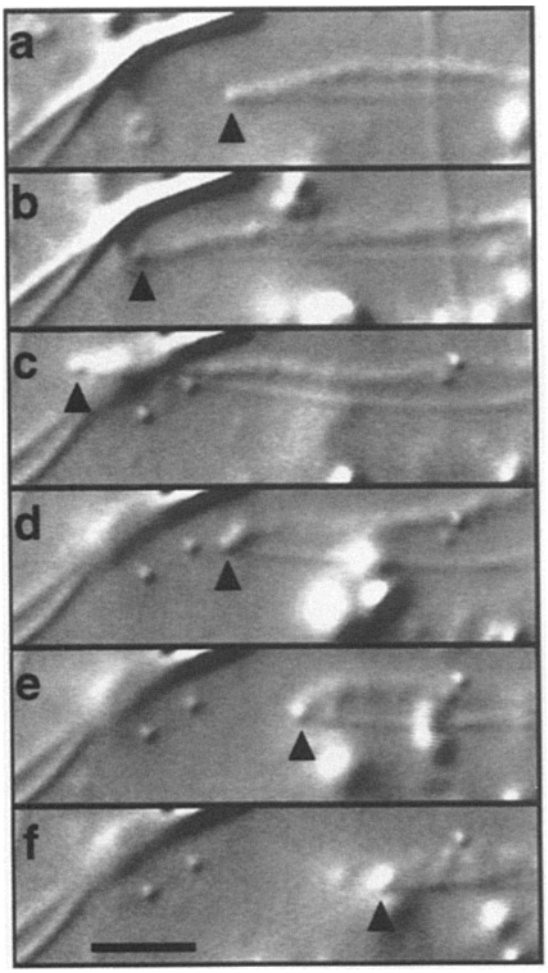

Figure 4. The membrane/microtubule TAC remains attached during both growth and shortening at the microtubule plus end. (*a–c*) A membrane tubule was formed by a TAC (*arrowhead*) as the microtubule elongated. (*d–f*) When the microtubule switched from growth to shortening, the attachment remained, and the membrane tubule was pulled back as the microtubule shortened at ~50 μm/min. Extract was made 5 mM AMP-PNP. Time: (*a*) 0 s; (*b*) 10 s; (*c*) 22 s; (*d*) 26 s; (*e*) 28 s; (*f*) 30 s. Bar, 2 μm.

back quickly (Fig 5 *c*), while the microtubule recoiled and straightened more slowly and continued its growth.

We also observed that the TACs had a strong affinity for the depolymerizing ends of microtubules. In a few cases, as a membrane tubule was being pulled by its attachment to a shortening microtubule, it became fixed at a point along its length by entanglement in the microtubule mesh. As the microtubule continued to shorten, the membrane became taut and stretched, exerting tensile force on the microtubule. When the membrane tubule became very resistant to further stretching, the TAC suddenly detached, and the membrane tubule recoiled back into an aggregate near its attachment site to the coverslip (not shown).

Estimates of the force required for TAC detachment from polymerizing ends were made from situations in which a stretched membrane induced a 90° angle between it and the axis of the microtubule end as the microtubule grew under compressive force (as in Fig. 5 *b*). In this situation, the force of detachment is equal to the flexural rigidity of the microtubule divided by the radius of induced bend squared. When values of flexural rigidity reported for MAP-free microtubules assembled in vitro are used as an estimate (in the range of 0.8–5 $\times$ 10^{-23} Nm^2; Dye et al., 1993; Gittes et al., 1993; Venier et al., 1994; Tran, P., M. P. Sheetz, and E. D. Salmon, personal observations), we calculated a value for the detachment force in the range of 0.2 to 1.0 pN for radius of curvature between 5 and 10 μm. It was not possible to obtain a more precise measurement of the TAC detachment force since exact values for microtubule flexual rigidity and the elastic properties of the membranes in the extract are unknown.

Discussion

The two most interesting findings of the present study are that: (*a*) the ER, and possibly other types of unidentified membranes in the *Xenopus* cytoplasm contain TACs that are able to stay attached to microtubule plus ends during both the growth and shortening states of dynamic instability without altering the kinetics of tubulin association/dissociation; and (*b*) TAC motility is generated by plus end polymerization/depolymerization dynamics by a mechanism insensitive to inhibitors of motility produced by conventional kinesins or dynein. In this regard, it is important to consider both the molecular nature and mechanism of TAC motility, as well as the possibility that this type of motility is involved in organelle movement in the cell.

The Membrane/Microtubule TAC: Molecular Candidates

The dynamics of attachment of the TAC to the microtubule dimer lattice at polymerizing and depolymerizing ends is defined by the velocites of growth and shortening. For example, at a growth rate of 20 μm/min, dimer addition to the plus end occurs at 540 dimers/s. At a shortening rate of 60 μm/min, dimer dissociation occurs at 1620 dimers/s. During this rapid association or dissociation of dimers, the TAC must be able to maintain a robust association with the microtubule end without detachment, and without affecting normal rates of dimer exchange. Thus, it is likely that TAC attachment to a plus end is the collective result of many attachment molecules that interact transiently (weakly) and asychronously with binding sites on the 13 protofilaments in the microtubule cylindrical lattice.

In spite of the fact that membrane tubule formation by TACs was insensitive to inhibitors of microtubule motor ATPase activity, motor proteins still may be potential candidates for the molecules that dynamically link TACs to plus ends, as proposed earlier for kinetochore attachment to the plus ends of kinetochore microtubules (Koshland et al., 1988; Chandra et al., 1993; Skibbens et al., 1993; Lombillo et al., 1995*a, b*; Desai and Mitchison, 1995). One possibility is that the structure of the microtubule tip, i.e., the GTP-tubulin cap during growth, or the curled GDP-tubulin protofilaments during shortening, inactivates motor activity. Another possibility is that the attachment molecules are modified motor proteins not capable of active translocation. Dynein in the presence of vanadate and ATP (Vale et al., 1989), bacterially expressed constructs of the kinesin-like protein, ncd, (Chandra et al., 1993), and a chimera

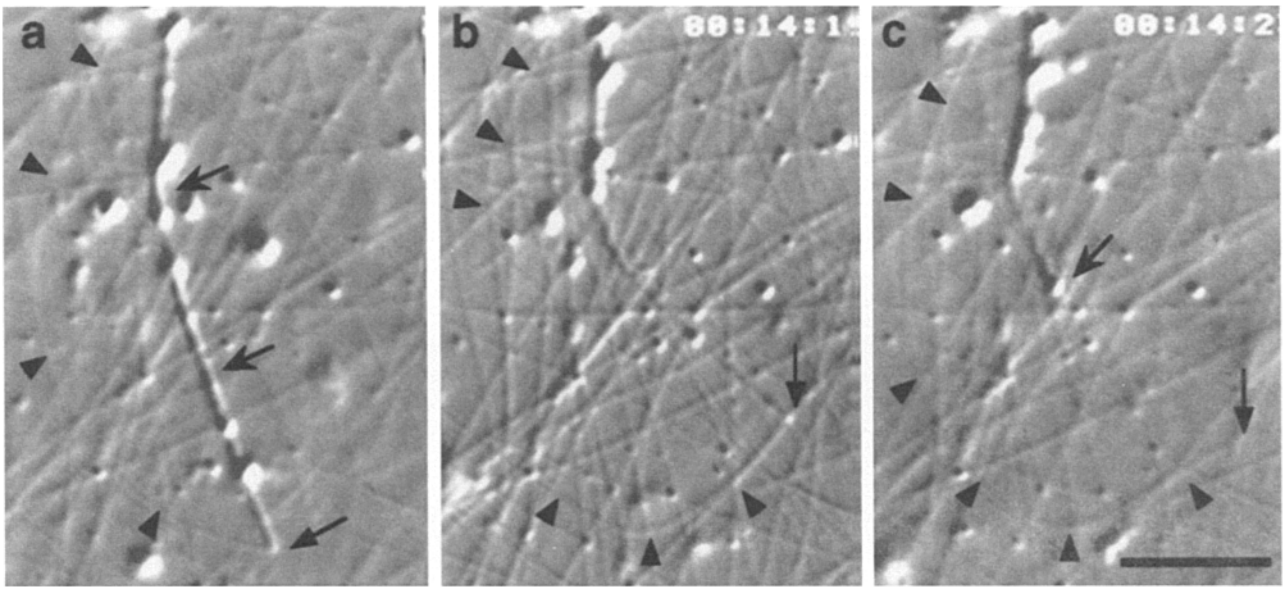

Figure 5. The membrane/microtubule TAC makes a fairly robust attachment to the microtubule tip in undiluted extract. (*a*) As a membrane tubule (*large arrows*) was formed by a growing microtubule (*arrowheads*), a region of the membrane tubule became stuck distal to its site of attachment at the microtubule tip (*small arrow*). As the microtubule continued to elongate, the membrane was pulled to its elastic limit. With continued microtubule growth, the microtubule bent and bowed (*arrowheads*) under the compressive force of the attached membrane. (*b*) The compressive force of the membrane and entanglement with other microtubules induced nearly a 180° bowing in the microtubule (*arrowheads*) and the taut membrane tubule (*arrow*) became oriented at nearly a 90° angle to the direction of microtubule growth. (*c*) The membrane tubule (*large arrows*) snapped off of the microtubule tip (*small arrow*) and rapidly recoiled within 0.2 s, while the free microtubule (*arrowheads*) straightened out much more slowly and continued growth along a linear path. Time: (*a*) 0 s; (*b*) 16 s; (*c*) 20 s. Bar, 2 μm.

of ncd tail and kinesin motor domains (Lombillo et al., 1995*b*) are all capable of binding to microtubules in a "weak," non-force generating state independent of ATP hydrolysis. These molecules have been shown to maintain attachment to the microtubule lattice while permitting longitudinal displacements along the lattice driven by Brownian motion. Also, kinesins in a weak binding state are capable of coupling a bead or a kinetochore to the end of a depolymerizing microtubule both in the presence or absence of ATP (Lombillo et al., 1995*a, b*). Whether kinesins work equally well at maintaining attachment to the tip of polymerizing ends is unknown.

Alternatively, the attachment molecules may be non-motor microtubule binding proteins. This would explain why TAC motility was insensitive to inhibitors of motor activity in our studies. One potential molecular candidate is the microtubule binding protein, CLIP-170. This protein is concentrated at the plus ends of microtubules in interphase cells and can function to couple membranes to microtubules (Scheel and Kreis, 1991; Pierre et al., 1992).

Polymerization/Depolymerization Driven Force Production

An important aspect of our experimental results is that they demonstrate that an individual microtubule plus end can push during the growth phase and pull during the shortening phase of dynamic instability. These findings add to the list of evidence that demonstrates that the assembly dynamics of cytoskeletal filaments can contribute significant pushing or pulling forces for cellular motility (Tilney and Inoue, 1982; Koshland et al., 1988; Miyamoto and Hotani, 1988; Cortese et al., 1989; Dabiri et al., 1990; Coue et al., 1991; Theriot and Mitchison, 1991; Janmey et al., 1992; Miyata and Hotani, 1992; Sanger et al., 1992; Theriot et al., 1992; Lombillo et al., 1995*a, b*). The mechanism of force generation for TAC motility during tubulin dimer association/disassociation at the microtubule end is probably some type of "Brownian ratchet" (Hill, 1985; Peskin et al., 1993; Desai and Mitchison, 1995; Oster et al., 1995). It is also likely that growth and shortening of plus ends can generate much more force than the drag forces on the membranes in the extract, since TAC attachment did not significantly affect the kinetics of tip growth or shortening. However, the strength of membrane attachment to the microtubule tip during growth and shortening may substantially limit the useful force that can be generated by assembly/disassembly. Direct measurements of native microtubule flexural rigidity and the forces that stall plus end growth and shortening are needed to be certain of the TAC detachment force and the potential force generation by tubulin assembly dynamics.

Implications for TACs In Vivo

Our demonstration in *Xenopus* extracts that the assembly/dissassembly dynamics of microtubules are able to drive the formation of tubular membrane networks suggests that membrane/microtubule TACs may contribute to the formation of tubulovesicular organelle systems in the cell. The membrane tubules and polygonal networks formed by TACs in our in vitro system are similar in structure to both

the ER and Golgi apparatus in living cells (Terasaki et al., 1984, 1986; Lee and Chen, 1988; Dailey and Bridgman, 1989; Lee et al., 1989; Cooper et al., 1990). Although both membrane and microtubule dynamics have not been observed simultaneously in living cells, there is morphological evidence suggesting that TACs may contribute to the construction and maintenance of organelles. For example, in whole mount EM of advancing neuronal growth cones, where both the tubulovesicular and microtubule networks are relatively sparse (Dailey and Bridgman, 1989), the co-termination of membrane tubules and microtubules is striking. Similar to the TAC, the termini of these membrane tubules are characterized by a globular, bulblike domain (Dailey and Bridgman, 1991).

In living cells, the extension of tubulovesicular processes is marked by linear advance that is often interrupted by periods of retreat and recovery (Lee and Chen, 1988; Cooper et al., 1990). Although this type of behavior has been observed in vitro during tubule formation via gliding mechanisms (Dabora and Sheetz, 1988), it is also characteristic of microtubule ends undergoing dynamic instability observed both in vitro (Walker et al., 1988) and in living cells (Cassimeris et al., 1988; Sammak and Borisy, 1988; Shelden and Wadsworth, 1993). In cells, tubulovesicular elements of the Golgi apparatus extend at a maximum rate of ~24 μm/min (Cooper et al., 1990), while ER tubules extend at up to ~70 μm/min (Lee and Chen, 1988). The rate of Golgi tubule extension in vivo is similar to the membrane tubule elongation rates we observed for TAC coupled growing microtubules in our undiluted *Xenopus* extracts (19.05 μm/min) and to the rates of growth of microtubule plus ends in mammalian interphase cells in culture (~20 μm/min) (Shelden and Wadsworth, 1993). However, we did not determine if Golgi-derived membranes were present in the networks formed in our system.

These comparisons to available in vivo data suggest that membrane/microtubule TAC motility and microtubule motor activity can both contribute to the formation of tubulovesicular organelle systems. This is supported by our observation that membrane tubule formation may occur in diluted *Xenopus* egg extract by two distinct mechanisms: either by membrane gliding, or by TAC motility. Similar to the variety of functional roles played by microtubule motors, TAC-like attachments to other organelles or structures in cells may also couple microtubule plus end assembly dynamics to force production for several different microtubule dependent motile phenomena. Examples include kinetochore motility during prometaphase congression and anaphase segregation (Coue et al., 1991; Skibbens et al., 1993; Lombillo et al., 1995*b*), poleward flux of kinetochore fiber microtubules (Mitchison, 1990; Sawin and Mitchison, 1991; Mitchison and Salmon, 1992), anaphase B spindle elongation in vertebrate cells (Waters et al., 1993) and yeast (Yeh et al., 1995), and the movement and the tethering of spindles to specific sites at the cell surface during the asymmetrical divisions of oocyte meiosis and embryonic development (Hyman and White, 1987; Lutz et al., 1988).

This work is based on observations that were originally made at Woods Hole Marine Biological Laboratory Physiology course in the summer of 1993. The authors wish to acknowledge the faculty, students, and staff members of this class for their support and enthusiasm. In particular, A. W. Murray, D. Frank, C. Zhu, R. Skibbens and T. D. Pollard. We also thank L. Cassimeris, E. L. F. Holzbaur, T. Yen, S. Inoue, M. Terasaki, S. Zigmond, and G. Oster for their insightful comments, and C. Nicchita for rough ER fractions and ER specific antibodies.

This work is supported by National Institutes of Health (NIH) GM31136-14 to the MBL Physiology Course, and NIH GM24364 to E. D. Salmon. C. M. Waterman-Storer is supported by predoctoral fellowships from the American Heart Association and Pennsylvania Muscle Institute (NIH T32-AR07584-01).

Received for publication 2 February 1995 and in revised form 26 May 1995.

References

Allan, V. J., and R. D. Vale. 1991. Cell cycle control of microtubule-based transport and tubule formation in vitro. *J. Cell Biol.* 113:347–359.

Allan, V. J., and R. D. Vale. 1994. Movement of membrane tubules along microtubules in vitro: evidence for specialized sites of motor attachment. *J. Cell Sci.* 107:1885–1897.

Bell, C. W., C. Fraser, W. S. Sale, W.-J. Y. Tang, and I. R. Gibbons. 1982. Preparation and purification of dynein. *J. Cell Biol.* 24:373–397.

Belmont, L. D., A. A. Hyman, K. E. Sawin, and T. J. Mitchison. 1990. Real-time visualization of cell cycle-dependent changes in microtubule dynamics in cytoplasmic extracts. *Cell.* 62:579–589.

Caplow, M. 1992. Microtubule dynamics. *Curr.Opin. Cell Biol.* 4:58–65.

Cassimeris, L., N. K. Pryer, and E. D. Salmon. 1988. Real-time observations of microtubule dynamic instability in living cells. *J. Cell Biol.* 107:2223–2231.

Chandra, R., S. Endow, and E. D. Salmon. 1993. An N-terminal truncation of the ncd motor protein supports diffusional movement of microtubules in motility assays. *J. Cell Sci.* 104:899–906.

Cooper, M. S., A. Cornell-Bell, A. Chernjavsky, J. W. Dani, and S. J. Smith. 1990. Tubulovesicular processes emerge from trans-Golgi cisternae, extend along microtubules, and interlink adjacent trans Golgi elements into a reticulum. *Cell.* 61:135–145.

Cortese, J. D., B. Schwab, C. Friden, and E. L. Elson. 1989. Actin polymerization induces shape change in actin containing vesicles. *Proc. Nat. Acad. Sci. USA.* 86:5773–5777.

Coue, M., V. A. Lombillo, and J. R. McIntosh. 1991. Microtubule depolymerization promotes particle and chromosome movement in vitro. *J. Cell Biol.* 112:1165–1175.

Dabiri, G. A., J. M. Sanger, D. A. Portnoy, and F. S. Southwick. 1990. Listeria monocytogenes moves rapidly through host cell cytoplasm by inducing directional actin assembly. *Proc. Nat. Acad. Sci. USA.* 87:6068–6072.

Dabora, S. L., and M. P. Sheetz. 1988. Microtubule dependent formation of a tubular vesicular network with characteristics of the endoplasmic reticulum from cultured cell extracts. *Cell.* 54:27–35.

Dailey, M. E., and P. C. Bridgman. 1989. Dynamics of the endoplasmic reticulum and other membranous organelles in growth cones of cultured neurons. *J. Neurosci.* 9:1897–1909.

Dailey, M. E., and P. C. Bridgman. 1991. Structure and organization of membrane organelles along distal microtubule segments in growth cones. *J. Neurosci. Res.* 30:242–258.

Desai, A., and T. Mitchison. 1995. A new role for motor proteins as couplers to depolymerizing microtubules. *J. Cell Biol.* 128:1–4.

Drechsel, D. N., and M. W. Kirschner. 1994. The minimum GTP cap required to stabilize microtubules. *Curr. Biol.* 4:1053–1061.

Dye, R. B., S. P. Fink, and R. C. Williams, Jr. 1993. Taxol-induced flexibility of microtubules and its reversal by MAP-2 and Tau. *J. Biol. Chem.* 268:6847–6850.

Erickson, H. P., and T. O'Brien. 1992. Microtubule dynamic instability and GTP hydrolysis. *Annu. Rev. Biophys. Biomol. Struct.* 21:145–166.

Gard, D. L., and M. W. Kirschner. 1987. Microtubule assembly in cytoplasmic extracts of *Xenopus* oocytes and eggs. *J. Cell Biol.* 105:2191–2201.

Gittes, F., B. Mickey, J. Nettleton, and J. Howard. 1993. Flexural rigidity of microtubules and actin filaments measured from thermal fluctuations in shape. *J. Cell Biol.* 120:923–934.

Gorlich, D., S. Prehn, E. Hartman, K. U. Kalies, and T. A. Rapoport. 1992. A mammalian homolog of SEC61p and SECYp is associated with ribosomes and nascent polypeptides during translation. *Cell.* 71:489–503.

Hill, T. L. 1985. Theoretical problems related to the attachment of microtubules to kinetochores. *Proc. Natl. Acad. Sci. USA.* 82:4404–4408.

Hyman, A. A., D. Cretien, I. Arnal, and R. H. Wade. 1995. Structural changes accompaning GTP hydrolysis in microtubules: information from a slowly hydrolyzable analogue Guanylyl-(a,b)-Methylene-Diphosphonate. *J. Cell Biol.* 128:117–125.

Janmey, P, C. Cunningham, G. Oster, and T. Stossel. 1992. Cytoskeletal networks and osmotic pressure in relation to cell structure and motility. *In* Swelling Mechanics: From Clays to Living Cells and Tissues. T. Karalis, editor. Springer Verlag, Heidelberg. 333–346.

Koshland, D. E., T. J. Mitchison, and M. W. Kirschner. 1988. Polewards chromosome movement driven by microtubule depolymerization in vitro. *Nature*

(Lond.). 331:499–504.
Lee, C., and L. B. Chen. 1988. Dynamic behavior of endoplasmic reticulum in living cells. *Cell.* 54:37–46.
Lee, C., M. Ferguson, and L. B. Chen. 1989. Construction of the endoplasmic reticulum. *J. Cell Biol.* 109:2045–2055.
Lombillo, V. A., R. J. Stewart, and J. R. McIntosh. 1995*a*. Minus-end-directed motion of kinesin-coated microspheres driven by microtubule depolymerization. *Nature (Lond.)*. 373:161–164.
Lombillo, V. A., C. Nislow, T. J. Yen, V. I. Gelfand, and J. R. McIntosh. 1995*b*. Antibodies to the kinesin motor domain and CENP-E inhibit microtubule depolymerization-dependent motion of chromosomes in vitro. *J. Cell Biol.* 128:107–115.
Lutz, D. A., Y. Hamaguchi, and S. Inoue. 1988. Micromanipulation studies of the asymmetric positioning of the maturation spindle in *Chaetopterus sp.* oocytes: I. Anchorage of the spindle to the cortex and migration of a displaced spindle. *Cell Motil. Cytoskeleton.* 11:83–96.
Mitchison, T. J. 1990. Polewards microtubule flux in the mitotic spindle: evidence from photoactivation of fluorescence. *J. Cell Biol.* 109:637–652.
Mitchison, T. J., and E. D. Salmon. 1992. Poleward kinetochore fiber movement occurs during both metaphase and anaphase-A in newt lung cell mitosis. *J. Cell Biol.* 119:569–582.
Miyamoto, H., and H. Hotani. 1988. Polymerization of microtubules within liposomes produces morphological change of their shapes. *Proc. Tanaguchi Int. Symp.* 14:220–242.
Miyata, H., and H. Hotani. 1992. Morphological changes in liposomes caused by polymerization of encapsulated actin and spontaneous formation of actin bundles. *Proc. Nat. Acad. Sci. USA* . 89:11547–11551.
Munro, S., and H. R. Pelham. 1986. An HSP70-like protein in the ER: identity with the 78 kDa glucose-regulated protein and immunoglobulin heavy chain binding protein. *Cell.* 46:291–300.
Murray, A. W. 1991. Cell cycle extracts. *Methods Cell Biol.* 36:581–609.
Oster, G., C. S. Peskin, and V. Lombillo. 1995. A depolymerization ratchet for intracellular transport. *In* Fluctuations and Order: The New Synthesis. M. Millonas, Editor. Springer Verlag, NY. In press.
Peskin, C. S., G. M. Odell, and G. F. Oster. 1993. Cellular motions and thermal fluctuations: The Brownian ratchet. *Biophys. J.* 65:316–324.
Pierre P., J. Scheel, J. E. Rickard, and T. E. Kreis. 1992. CLIP-170 links endocytic vesicles to microtubules. *Cell.* 70:887–900.
Rieder C. L., and E. D. Salmon. 1994. Motile kinetochores and polar ejection forces dictate chromosome position on the vertebrate mitotic spindle. *J. Cell Biol.* 124:223–233.
Rosenfeld, M. G., E. E. Marcantonio, J. Hakimi, V. M. Ortt, P. H. Atkinson, D. Sabatini, and G. Kreibich. 1984. Biosynthesis and processing of ribophorins in the endoplasmic reticulum. *J.Cell Biol.* 99:1076–1082.
Salmon, E. D., T. Inoue, A. Desai, and A. W. Murray. 1994. High resolution multimode digital imaging system for mitosis studies in vivo and in vitro. *Biol Bull.* 187:231–232.
Sammak, P. J., and G. Borisy. 1988. Direct observation of microtubule dynamics in living cells. *Nature (Lond.)*. 332:724–726.
Sanger, J. M, J. W. Sanger, and F. S. Southwick. 1992. Host cell actin assembly is necessary and likely to provide the propulsive force for intracellular movement of listeria monocytogenes. *Infect. Immun.* 60:3609–3619.
Scheel, J., and T. E. Kreis. 1991. Motor protein independent binding of endocytic carrier vesicles to microtubules in vitro. *J. Biol. Chem.* 266:18141–18148.
Sawin, K., and T. J. Mitchison. 1991. Poleward flux in mitotic spindles assembled in vitro. *J. Cell Biol.* 112:941–954.
Shelden, E., and P. Wadsworth. 1993. Observation and quantification of individual microtubule behavior in vivo: microtubule dynamics are cell-type specific. *J. Cell Biol.* 120:935–945.
Skibbens, R. V., V. P. Skeen, and E. D. Salmon. 1993. Directional instability of kinetochore motility during chromosome congression and segregation in mitotic newt lung cells: a push-pull mechanism. *J. Cell Biol.* 122:859–875.
Terasaki, M., and T. S. Reese. 1994. Interactions among endoplasmic reticulum, microtubules, and retrograde movements on the cell surface. *Cell Motil. Cytoskeleton.* 29:291–300.
Terasaki, M., J. Song, J. R. Wong, M. J. Weiss, and L. B. Chen. 1984. Localization of endoplasmic reticulum in living and glutaraldehyde-fixed cells with fluorescent dyes. *Cell.* 38:101–108.
Terasaki, M., L. B. Chen, and K. Fujiwara. 1986. Microtubules and the endoplasmic reticulum are highly interdependent structures. *J. Cell Biol.* 103: 1557–1568.
Theriot, J. A., and T. J. Mitchison. 1991. Actin microfilament dynamics in locomoting cells. *Nature (Lond.)*. 352:126–131.
Theriot, J. A., T. J. Mitchison, L. G. Tilney, and D. A. Portnoy. 1992. The rate of actin-based motility of *Listeria monocytogenes* equals the rate of actin polymerization. *Nature (Lond.)*. 357:257–260.
Tilney, L., and S. Inoue. 1982. The acrosomal reaction of *Thyone* sperm. II: the kinetics and possible mechanism of acrosomal process elongation. *J. Cell Biol.* 93:820–827.
Vale, R. D., and H. Hotani. 1988. Formation of membrane networks in vitro by kinesin-driven microtubule movement. *J. Cell Biol.* 107:2233–2241.
Vale, R. D., D. R. Soll, and I. R. Gibbons. 1989. One dimensional diffusion of microtubules bound to flagellar dynein. *Cell.* 59:915–925.
Venier, P., A. C. Maggs, M.-F. Carlier, and D. Pantaloni. 1994. Analysis of microtubule rigidity using hydrodynamic flow and thermal fluctuations. *J. Biol. Chem.* 269:13353–13360.
Verde, F., M. Dogterom, E. Stelzer, E. Karsenti, and S. Leibler. 1992. Control of microtubule dynamics and length by cyclin A- and cyclin B-dependent kinases in *Xenopus* egg extracts. *J. Cell Biol.* 118:1097–1108.
Walker, R., E. O'Brien, N. Pryer, M. Soboeiro, W. Voter, H. Erikson, and E. D. Salmon. 1988. Dynamic instability of individual microtubules analyzed by video light microscopy: rate constants and transition frequencies. *Cell.* 107: 1437–1448.
Waters, J. C., R. W. Cole, and C. L. Rieder. 1993. The force producing mechanism for centrosome separation during spindle formation is intrinsic to each aster. *J. Cell Biol.* 122:361–372.
Yeh, E., R. V. Skibbens, J. W. Cheng, E. D. Salmon, and K. Bloom. 1995. Spindle dynamics and cell cycle regulation of dynein in the budding yeast *Saccharomyces cerevisiae*. *J. Cell Biol.* 130:687–700.